Random insertion of GFP into the cAMP-dependent protein kinase regulatory subunit from *Dictyostelium discoideum*

Ricardo M. Biondi, Pascal J. Baehler[1], Christophe D. Reymond[1],* and Michel Véron

Unité de Régulation Enzymatique des Activités Cellulaires, CNRS-URA 1773, Institut Pasteur, 25 rue du Dr Roux, 75724, Paris Cedex 15, France and [1]Institut de Biologie Cellulaire et de Morphologie, Université de Lausanne, rue du Bugnon 9, CH-1005 Lausanne, Switzerland

ABSTRACT

The green fluorescent protein (GFP) is currently being used for diverse cellular biology approaches, mainly as a protein tag or to monitor gene expression. Recently it has been shown that GFP can also be used to monitor the activation of second messenger pathways by the use of fluorescence resonance energy transfer (FRET) between two different GFP mutants fused to a Ca^{2+} sensor. We show here that GFP fusions can also be used to obtain information on regions essential for protein function. As FRET requires the two GFPs to be very close, N- or C-terminal fusion proteins will not generally produce FRET between two interacting proteins. In order to increase the probability of FRET, we decided to study the effect of random insertion of two GFP mutants into a protein of interest. We describe here a methodology for random insertion of GFP into the cAMP-dependent protein kinase regulatory subunit using a bacterial expression vector. The selection and analysis of 120 green fluorescent colonies revealed that the insertions were distributed throughout the R coding region. 14 R/GFP fusion proteins were partially purified and characterized for cAMP binding, fluorescence and ability to inhibit PKA catalytic activity. This study reveals that GFP insertion only moderately disturbed the overall folding of the protein or the proper folding of another domain of the protein, as tested by cAMP binding capacity. Furthermore, three R subunits out of 14, which harbour a GFP inserted in the cAMP binding site B, inhibit PKA catalytic subunit in a cAMP-dependent manner. Random insertion of GFP within the R subunit sets the path to develop two-component FRET with the C subunit.

INTRODUCTION

Since it was first cloned in 1992 (1), the green fluorescent protein (GFP) from the jellyfish *Aequorea victoria* has been used in many *in vivo* cell biology approaches to monitor the localization of GFP fused to proteins of interest (2) or promoter activation (3). The versatility of this technique has been enlarged by the production of multiple mutants with different fluorescence spectra (4). The green fluorescence of GFP was recently extended to monitor physiological changes as an indirect or direct measure of enzyme activities. Thus, constructs have been developed to produce fusion proteins where two GFPs, a donor and an acceptor with overlapping absorption and emission spectra, allow to sense intracellular Ca^{2+} levels by means of fluorescence resonance energy transfer (FRET) changes (5,6). The appearance or disappearance of FRET reflects the distance (*d*) between the GFPs since FRETs efficiency decreases as a function of d^6.

PKA is composed of regulatory (R) and catalytic (C) subunits which associate in an inactive holoenzyme. The R subunit has two cAMP binding sites named site A and site B, which display different binding properties towards cAMP (7). Upon binding of cAMP to the R subunit, the holoenzyme dissociates, liberating active C subunits. PKA thus represents a sensitive indicator of intracellular cAMP levels. By microinjecting purified mammalian R and C subunits labelled with two different chemical fluorochromes, PKA was used to follow changes in intracellular cAMP concentration *in vivo* by FRET disappearance upon stimulation of smooth muscle and fibroblast cell lines with β-adrenergic agonists or prostaglandin E1 (8).

In *Dictyostelium*, PKA is also made of R and C subunits. However, both subunits display some structural differences with their mammalian counterparts. The R subunit lacks a dimerization domain present at the N-terminus of mammalian regulatory subunits and accordingly, the holoenzyme forms an RC dimer rather than the usual R_2C_2 tetramer (9). The C subunit has an additional domain at its N-terminus whose function begins to be established (10,11).

FRET between two different GFPs fused with the R and C subunits when the subunits are associated within the holoenzyme would be of obvious interest, both to measure *in vivo* variations of intracellular cAMP concentrations and to analyse the state of dissociation of the holoenzyme in various physiological conditions. However, N- or C-terminus GFP fusions did not bring the GFPs into close proximity so that FRET can occur. To avoid this problem, we decided to insert GFPs at random inside the coding region of the PKA R subunit from *Dictyostelium*. Here we describe the methodology used to produce these random insertions and the analysis of some of the R/GFP fusion proteins. The modification of the biochemical properties of certain R/GFP

*To whom correspondence should be addressed. Tel: +41 21 692 52 71; Fax: +41 21 692 52 75; Email: christophe.reymond@ibcm.unil.ch

The authors wish it to be known that, in their opinion, the first two authors should be regarded as joint First Authors

fusion proteins indicate that such insertions can provide useful functional mapping information.

MATERIALS AND METHODS

Materials

The plasmid pRSETb-R was described previously (10). *Escherichia coli* strain BL21 (DE3) was from Stratagene. Restriction and modification enzymes used were from Boehringer Mannheim, Promega, Pharmacia or Gibco. NTPs and protease inhibitor cocktail were from Boehringer Mannheim. CsCl was from Sigma. Monoclonal anti-His-tag antibodies were from Qiagen. Monoclonal antibodies anti-R111, from cell culture supernatants, were a kind gift of Prof. Gerisch (Max Planck Institut, Martinsried, Germany). [^{3}H]cAMP, the ECL chemioluminescence kit used for western blot detection and ^{125}I-labelled secondary antibody used for protein quantification were from Amersham. Western blot quantification results were analysed using an Instant-Imager (Packard). Prestained protein molecular weight standards for SDS–PAGE (high) were from Gibco. The fluorescence microscope used for screening was an inverse Axiovert 25 (Zeiss) microscope with BP 450–490 excitation filter, beamsplitter FT510 and BP 515–565 emission filter (Zeiss). Fluorescence spectra were obtained with a PTI equipment and data were processed using Felix software. Plasmids containing S65T and W7 GFP mutant proteins, used as templates for PCR, were kindly provided by Dr R.Y.Tsien (University of California, San Diego, CA).

pRSETb-R/GFP library

The methodology used for the construction of the R/GFP library is similar to that described (12). Nicks were first introduced in supercoiled pRSETb-R by a controlled DNase I treatment under conditions for nick translation to take place and then submitted to nuclease S1 digestion before addition of linkers and GFP fragments. In preliminary assays, supercoiled pRSETb-R plasmid (25 µg) was incubated in 1× DNA pol I buffer (Promega) at 15°C with 5 pg DNase I in a final volume of 50 µl. In order to evaluate the extent of the appearance of nicked circular plasmids, aliquots from different incubation times (0, 15, 30 and 45 min) were subjected to electrophoresis on 0.9% agar gels in TAE buffer for 3–5 h at constant voltage (50 V). Incubation times were chosen so that 30–50% of the plasmids were nicked. In the preparative experiment, all volumes were increased 25 times and the reaction mixture was equilibrated at 15°C in the presence of 75 µM of each dNTP and 400 U DNA pol I. The reaction was then initiated by the addition of DNase I and stopped after 15 min with EDTA (25 mM final concentration). After CsCl gradient centrifugation to purify nicked circular plasmids, incubation times with nuclease S1 were also chosen so that ≤50% of the plasmids were linearized. Longer incubation times did not increase substantially the appearance of linearized plasmids, suggesting that nuclease S1 was mostly acting on already linear plasmids producing deletions, rather than on nicks. The ends of the linearized plasmids were filled using T4 DNA polymerase to produce blunt ends to which *Sal*I linkers (gtcgac) were ligated. Either S65T or W7 GFP (4) fragments were amplified by 30 cycles of PCR using the primers 5′-CCCGTCGTCGACATG-AGTAAAGGAGAAGAA-3′ and 5′-AGTCGGGTCGACTTTG-TATAGTTCATCCATGCC-3′ with 1 min incubations at 95, 45 and 74°C for melting, annealing and elongation, respectively. Finally, *Sal*I-digested plasmids and PCR fragments were ligated

and plasmids were transformed in *E.coli* BL21 (DE3) by electroporation.

Functional screening of green fluorescent fusion proteins

Clones producing R/GFP fusion proteins were screened for fluorescence on agar plates, either directly by eye observation in daylight or using an inverted microscope with fluorescein filters. Approximately $2–5 \times 10^5$ colonies were screened, allowing us to isolate 120 clones showing pRSETb-R/GFP fusions as seen by restriction mapping using either *Eco*RI to verify for the insertion of GFP or the combination of *Xho*I/*Sal*I or *Hin*dIII/*Sal*I to localize the approximate site of insertion.

In order to identify the GFP insertion sites within the R subunit sequence, two primers from the GFP coding regions were designed and used to sequence in the 3′ and 5′ direction from the GFP gene. The primers used were 5′-GCTGCTGGGATTACACA-3′ and 5′-TAACATCACCATCTAAT-3′.

Fluorescence spectra

The assay was performed at 20°C using variable amounts of total cell suspensions or partially purified proteins in 50 mM Tris–HCl, pH 7.5. Bandwidths were kept constant at 6 nm. Integration time was usually 0.2 s. Excitation and emission wavelengths used for GFP S65T were 490 and 510 nm and 450 and 510 nm for GFP W7.

Partial purification of R/GFP fusion proteins

Cells were grown at 37°C until OD$_{600}$ 0.3–0.6, induced for expression of the fusion protein with the addition of 1 mM IPTG and further incubated overnight at 22°C. R/GFP purifications were performed at 4°C. The cells from 500 ml cultures were broken in a French press in buffer A (50 mM Tris–HCl, pH 7.5, 100 mM NaCl, 0.1 mM DTT) in the presence of protease inhibitor cocktail. The extracts were immediately incubated with 0.5 ml Ni–agarose resin for 1 h. The resins were then loaded into columns and washed with 10 vol 5 mM imidazole in buffer A. In order to strip R subunits from any bound cAMP, the columns were washed with 5 vol 5 mM cGMP in buffer A at 0.5 ml/h, left overnight in the presence of cGMP and then extensively washed again with 5 mM imidazole in buffer A to remove cGMP. R/GFP fusion proteins were eluted using 100 mM imidazole in buffer A and extensively dialysed against buffer A to remove imidazole. R/GFP concentration in most of the partially purified samples was quantified by western blot using anti-R111 monoclonal antibody and ^{125}I-labelled secondary antibody; an instant imager was used to measure radioactivity associated with each band. For R/GFP 16 and R/GFP 106, quantification was performed on Coomassie blue stained SDS–PAGE gels. We estimated that this quantification was accurate within 30%, which was sufficient for the purpose of the experiments reported here.

cAMP binding assay

cAMP binding assays were performed using the ammonium sulphate precipitation assay as described (13). Variable amounts of bacterial extracts or partially purified samples were incubated in a final volume of 100 µl containing 50 mM Tris–HCl, pH 6.8, 100 mM KCl, 100 µg/ml BSA, 1 mM DTT and 50 nM cAMP (45 µCi/nmol) unless otherwise indicated. Separation between free and bound cAMP was performed by filtration (13) after 2 h incubation on ice (4°C). The amount of crude extract or partially

purified protein used in a given assay was adjusted so that the binding was linear with the amount of sample used. For partially purified proteins, the measured radioactivity was at least 3-fold above background. For most clones, however, the specific binding measured was between 10 and 20 times background (Table 2). The specificity of the binding was indicated by the fact that when 1 mg/ml BSA and 5′-AMP (at a concentration 10× greater then cAMP) were added to the incubation mixture, no difference in cAMP binding was found. Duplicates in a given experiment agreed within 20%.

PKA activity assay

Cells were grown at 37°C until OD_{600} 0.3–0.6, induced for expression of fusion protein by addition of 1 mM IPTG and further incubated for 4 h at 28°C. An equivalent of 1 OD of cells were lysed at 4°C in 100 µl of HMN (50 mM HEPES, 40 mM $MgCl_2$, 20 mM NaCl, 0.5% NP-40) in the presence of protease inhibitors. For the extract of C309 (truncated version of the *Dictyostelium* C subunit), DEAE–Sephacel (Pharmacia) was added and binding was performed at 4°C for 30 min. After centrifugation, PKA C was eluted in high salt buffer (HMN with 200 mM KCl) at 4°C for 5 min.

PKA activity was measured using the PepTag™ kit from Promega with fluorescent peptide LRRASLG (derived from Kemptide) as a substrate according to the manufacturer's instructions. C and R subunits were mixed with or without cAMP. Enzymatic reactions were carried out at 20°C for 45 min. Phosphorylation by PKA alters the net charge of Kemptide from +1 to –1, so that the phosphorylated peptide can be separated from the unphosphorylated on buffered agarose gels.

RESULTS AND DISCUSSION

The methodology used for random insertion of GFP is a variation from that used by Luckow *et al*. (12) to make linker scanning mutants in the promoter of the chicken lysozyme gene. We produced nicks in the vector by incubating the PKA R expression plasmid along with DNase I, DNA pol I and dNTPs under the conditions where nick translation takes place. Then, a nuclease S1 treatment at pH 5.7 was used to linearize the plasmid at the position of the nicks. *Sal*I linkers were inserted and the plasmids were cut before cloning either S65T or W7 GFP mutants therein. After transforming BL21 (DE3) *E.coli* cells, green colonies were identified directly on agar plates and isolated. GFP insertion was verified by *Sal*I digestion of the purified plasmids. Using *Xho*I/*Sal*I and *Hin*dIII/*Sal*I digestions, we determined the approximate site of insertion of the GFP within plasmid pRSETb-R. About 50% of the plasmids showed GFP inserted outside of the R coding sequence, possibly due to the expression of GFP/AmpR fusion proteins. These clones were not further characterized.

One hundred and twenty clones with GFP inserted within the R subunit coding region were isolated. As shown in Figure 1, insertions occurred throughout the R coding sequence, indicating that the methodology indeed resulted in the random insertion of nicks. Since the colonies were selected on the basis of their green fluorescence, we expected GFP to be fused in-frame with the R coding sequence in all of the 120 clones shown in Figure 1. This does not preclude that the sequence of the R subunit located downstream of the GFP would be out of frame, due to small deletions that could have occurred during the nuclease S1 digestion.
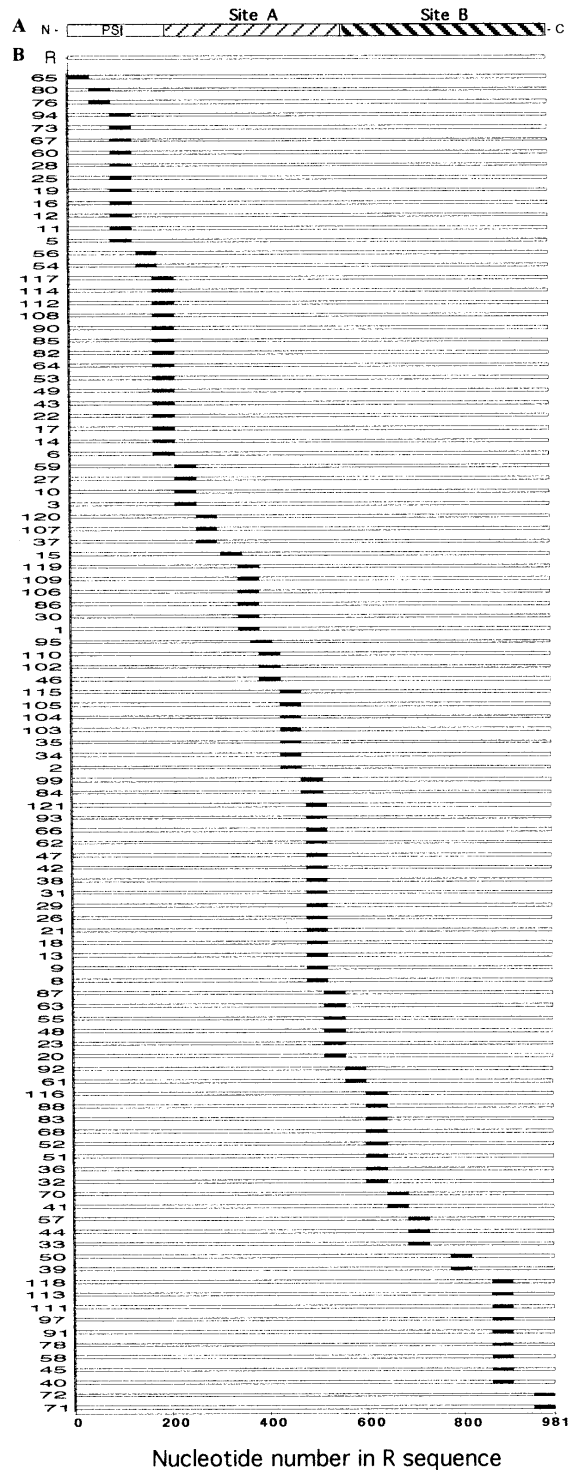
Figure 1. Location of the GFP insertion sites in R/GFP fusion plasmids. (**A**) A scheme of the *Dictyostelium* R subunit shows the position of the putative pseudo-substrate region (PS) and the cAMP binding sites A and B. For the sake of simplicity, the N-terminal His tag and enterokinase recognition sequence from plasmid pRSET-B (Invitrogen) are not shown. (**B**) To calculate the position of the GFP insertion site, purified plasmids were digested with combinations of two restriction enzymes, *Sal*I/*Xho*I and *Sal*I/*Hin*dIII, and separated by 1% agarose electrophoresis in TBE buffer. The position of the insertion sites were then calculated based on the size of the bands. The error on GFP insertion site was mostly found to be <50 bp. One hundred and seven individual R/GFP clones are represented; a black box comprising 40 nt shows the approximate GFP insertion site on each R/GFP clone.
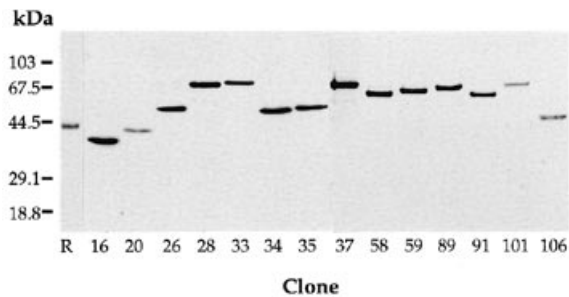
Figure 2. Western blot analysis of R/GFP green fluorescent clones. Extracts from 14 representative clones were separated by 12% SDS–PAGE. R/GFP fusion proteins were recognized by western blot with anti-His-tag antibodies. Clones with bands at 70–75 kDa were selected as potential in-frame constructs. The molecular weight markers are shown at the left side. The number on top of each lane refers to the corresponding R/GFP clone.

In order to screen for clones where GFP was fused in-frame with the complete R subunit, we performed western blots on extracts from the 120 clones. Figure 2 shows the analysis of a representative sample of clones as revealed using anti-His-tag antibodies. Thirty five clones showed fusion proteins between 70 and 75 kDa, approximately the size expected for a fusion between R and GFP (68 kDa). Typical examples of these are clones 28, 33, 37, 59, 89 and 101. Clones 58 and 91, although apparently also belonging to this group, were later found to encode truncated proteins at their C-terminus (below). Anti-R subunit antibodies were also used with similar results in most of the cases. Occasionally, however, two different bands were observed when using either anti-His-tag or anti-R antibodies. This could be due to colony contamination, degradation or to the presence of mixed plasmids in the original green fluorescent colony. A typical example is clone 20 for which anti-R antibodies revealed a band of 75 kDa indicating a full-length fusion protein (not shown), while a 40 kDa band was more strongly detected with anti-His-tag antibody (Fig. 2).

To determine the exact location of the GFP insertion, as well as the extent of deletions produced by the random insertion, we sequenced 23 clones selected from the western blot analysis. The

site of insertion as well as the extent of the deletion is shown in Figure 3 for 13 representative clones. We found that the extent of nucleotide deletions was low, varying in >80% of the cases (19/23) between 0 and 14 bp; in the remaining clones, deletions varied from 18 to 39 bp. Ten out of the 23 deletions contained only A/T nucleotides, corresponding, in total, to 78% of deleted nucleotides. The fact that in three clones GFP insertions took place within an exceptional 20 bp stretch of DNA composed of only A/T nucleotides, further indicated a bias for AT-rich sequences, which cannot be explained solely by the A/T richness of the *Dictyostelium* R sequence (68% A/T). Partial selectivity for A/T-rich regions could be either due to the nick translation or to the nuclease S1 treatment. The small deletions were most probably due to nuclease S1 digestion.

A drawback that we encountered after the screening step was due to the fact that some of the initially isolated colonies might have contained more than one plasmid. In addition, the extreme sensitivity of the GFP detection could have led to the selection of colonies where GFP could have been expressed in small amounts even if not in-frame with the R subunit. Thus, retransformation of R/GFP purified plasmids into BL21 (DE3) cells and reselection of stable green clones were performed to avoid the carry-over of unwanted plasmids and to eliminate clones not expressing fusion proteins. However, two clones escaped this screen and were found to fluoresce, although sequencing determined the presence of a GFP out of frame without a Met start codon in the proper reading frame.

We then asked whether the site of insertion could have an influence on the spectroscopic properties of the GFP. For this, both absorption and emission fluorescence spectra were recorded using bacterial cell suspensions of the 14 clones represented in Figure 2. As shown in Figure 4, in all but one clone, absorption and emission spectra superimposed with those of GFP S65T and GFP W7. In clone R/GFP W7-33, however, the emission spectrum was slightly (~10%) but significantly modified, showing a more intense peak at 503 nm than in the W7 GFP control, indicating a possible influence of this insertion site on GFP properties. (R/GFP fusion protein clones are either named by the

Clone

101	$^{31-}$gca aca gaa **AAA GTA GAA** gca caa aat^{-57}
20	$^{52-}$caa aat aat **AAT AAT A**tt aca cga aaa^{-78}
28	$^{139-}$att cca aaa **ACA GTA GAG ACA CAA CAA** nd
37	$^{199-}$ttt agt cat **TTA GAA GAG GAG GAA AGA AAC** gtt gta ttt tta^{-940}
59	$^{205-}$cat **TTA GAA GAG GAG GAA AGA AAC GTT GTA TTT TTA GCA ATG** gtt gaa^{-252}
106	$^{352-}$aat ggt ggt **∗** tcc cca act^{-371}
34	$^{493-}$tat aga cgt **ATA TTA ATG GAT CAA ACA ATT A**aa aag^{-528}
35	$^{493-}$tat aga cgt **ATA TTA A**tg gat caa^{-516}
26	$^{502-}$ata tta atg **G**at caa aca att aaa aag aga^{-531}
89	$^{514-}$caa aca att **AAA AAG** aga aaa tta^{-537}
33	$^{784-}$gaa att gca **TTA** ctt act gat aga^{-807}
91	$^{895-}$gat caa atg **CTT CGT CGT AAT At**g gaa act^{-924}
58	$^{916-}$atg gaa act **TA**t aat caa ttt^{-936}

Figure 3. Determination of the GFP insertion site by sequencing. The insertion sites of 13 representative clones (named by the R/GFP clone numbers on the left) were ordered by the location of the insertion site. To indicate the position of the insertion site, base pair numbers surrounding the deletions are indicated as superscripts. Bold upper case characters indicate nucleotides which were deleted upon insertion of GFP. In all clones GFP is in correct reading frame with the R-subunit. In clones 106, 34, 35, 26, 91 and 58, GFP insertion results in a frameshift, leading to stop codons at variable distances downstream from the GFP. The asterisk in clone 106 indicates a position where an adenine base was added after the second *Sal*I restriction site. nd indicates that for this clone, the extent of deletion has not been determined.
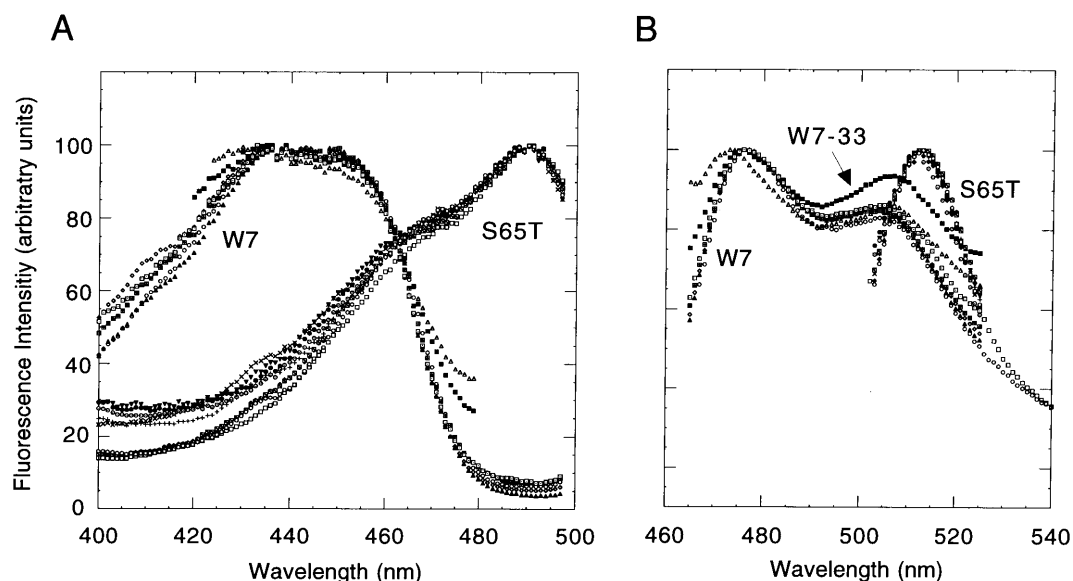
Figure 4. Fluorescence spectra of R/GFPs. Excitation (**A**) and emission (**B**) spectra were determined for GFP S65T, GFP W7 and for 15 different R/GFP clones containing either S65T or W7 GFP. The fluorescence of bacteria in suspension was recorded. In most cases, autofluorescence was negligible. Fluorescence intensity was normalized so that the highest intensity peaks corresponded to 100%. R/GFP clones shown are: S65T-12, S65T-16, W7-20, W7-26, S65T-28, W7-33, W7-34, S65T-35, S65T-37, S65T-58, W7-59, W7-89, W7-91, S65T-101, S65T-106.

clone number alone or by the name of GFP inserted followed by the clone number in cases where specification of the type of GFP is important, as for example, W7-33). cAMP addition was without effect on the fluorescent properties of any of the clones tested. As for fluorescence intensity, R/GFP S65T was in general found to have a stronger fluorescence than R/GFP W7. When W7 was replaced by S65T in several R/GFP clones, an ~5–10 times higher fluorescence intensity was observed in cell suspension (data not shown). As quantum yields of GFPs S65T and W7 are very similar (4), this result suggests that GFP W7 has additional folding constraints or is less stable when present as a fusion protein. On the other hand, no clear correlation could be established between the fluorescence intensity and insertion site. These variations possibly resulted from the sensitivity of GFP to proper folding dependent on time and temperature.

We then studied the effect of GFP insertion on the cAMP binding activity of the fusion proteins. In a first step, cAMP binding assays were performed using crude cell extracts from 93 different R/GFP clones expressing R/GFP fusion proteins. Fifty seven out of 93 clones had significant cAMP binding (not shown). At this point it should be noted that ~65% of the clones had C-terminal deletions due to frameshifts (above). For this reason, the lack of cAMP binding in the remaining 36 clones would not only be due to a conformational effect of GFP insertion into the cAMP binding site, but also to the deletion of the corresponding cAMP binding sites. Considering this, we estimated that only 14 clones had lost cAMP binding as a consequence of GFP insertion.

We next performed a more precise cAMP binding characterization on 14 clones already presented in Figure 2, for which the insertion site sequence had been characterized. The R/GFP fusion proteins were partially purified on Ni–agarose columns as described in Materials and Methods. In all cases, SDS–PAGE showed a prominent band corresponding to the fusion protein which was 10–90% pure, depending on the clone considered (not shown). The results of the cAMP binding assays are shown in
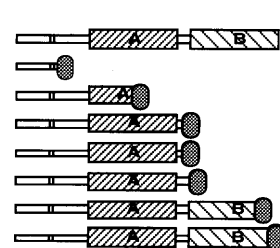
Tables 1 and 2 for two representative subsets of these clones. The cAMP binding values were normalized to similar protein concentrations after estimation of the latter by semi-quantitative western blots as described in Materials and Methods. Purified recombinant R subunit (10) was used as control and its cAMP binding set at 100%.

Table 1 shows the results obtained from clones in which the insertion of GFP resulted in a frameshift producing C-terminal deletions in the R subunit. Fusion proteins 16 and 106 showed very little or no cAMP binding, in accordance with the fact that their R subunit is deleted upstream from or within the cAMP binding site A (Fig. 1A gives a schematic representation of the R subunit). A second group, represented by clones 34, 35 and 26 with a full cAMP binding site A and a completely deleted site B, showed little variation in cAMP binding, as compared with the wild-type R subunit. Indeed, it should be noted that our method to measure protein concentration does not allow a determination with >30% accuracy.

In order to correlate the biochemical properties of the fusion proteins with the insertion site of GFP, we built a three-dimensional model of the two cAMP binding sites of *Dictyostelium* R subunit, based on the known structure of the mouse homologue protein (14). The GFP insertion sites, corresponding to the 11 sequenced clones comprised in the model, are shown in Figure 5. Interestingly, highest binding was observed in clones 34, 35 and 26 in the absence of Tyr197 (the homologue to Trp260 in mouse sequence) which docks the adenine ring of cAMP bound to site A. This is similar to the results obtained using a truncated form of bovine RI subunit, in which domain B was deleted (15). A mutant at this position was identified to be a dominant inhibitor of PKA by genetic mapping in RIα of S49 mouse lymphoma cells (16). Altogether, our results support the model where an aromatic residue at this position is not necessary for the binding of cAMP to site A. The dominant inhibitor phenotype of this mutant could rather be explained if this residue had an important participation

Table 1. cAMP binding of partially purified R/GFP truncated fusion proteins

Clone	[1]Insertion site (nt)	[1]Insertion site (aa)	[2]MW (kDa)	cAMP Binding (%)	
[3]R	–	–	40	100	
16	93	31	38	0	
106	360	120	44	0.13	
34	501	167	48	74	
35	501	167	48	87	
26	510	170	50	130	
91	903	301	64	27	
58	924	308	67	4	

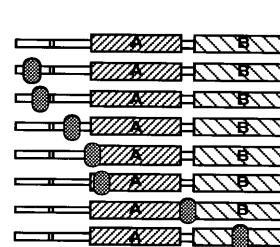[1]The insertion site is characterized by the last nucleotide or amino acid present before the deletion.
[2]Approximate molecular weights were estimated from western blots. Note that the estimated molecular weight of the R/GFP full-length protein is 68 kDa.
[3]R is the pure recombinant *Dictyostelium* R subunit.
[4]Scheme of the R subunit from *Dictyostelium* and R/GFP fusion proteins. GFP insertion is represented by an oval (not to scale).

Table 2. cAMP binding of partially purified in-frame R/GFP fusion proteins

Clone	[1]Insertion site (nt)	[1]Insertion site (aa)	[4]MW (kDa)	cAMP Binding (%)	
[2]R	–	–	40	100	
101	42	14	73	10	
20	60	20	75	3.0	
28	[3]147	49	70	1.3	
59	207	69	70	1	
37	228	76	75	2.3	
89	522	174	70	2.5	
33	792	264	70	15	

[1]The insertion site is characterized by the last nucleotide or amino acid present before the deletion.
[2]R is the pure recombinant *Dictyostelium* R subunit.
[3]Site of insertion only partially mapped, but the fusion protein has the expected size of 70 kDa.
[4]Approximate molecular weights were estimated from western blots.
[5]Scheme of the R subunit from *Dictyostelium* and R/GFP fusion proteins. GFP insertion is represented by an oval (not to scale).

in the conformational response of the protein to cAMP binding, as previously suggested (14).

The full-length fusion proteins (Table 2) showed, overall, a lower cAMP binding than purified R or truncated fusion proteins shown in Table 1, possibly linked to folding difficulties of such multidomain fusion proteins. Insertion of GFP within site A (clones 28, 59 and 37) significantly lowered cAMP binding as compared with clones 101 and 33, indicating a preferential binding of cAMP to site A. Due to the use of 50 nM cAMP we measured only high affinity binding. Thus these results indicate that, like in the mouse, the high affinity binding site of the PKA R from *Dictyostelium* is site A, which is in accordance with the high sequence conservation between mouse and *Dictyostelium*.

We did not attempt to determine precisely the K_D of cAMP for each of the isolated clones. Rather, we compared cAMP binding at two cAMP concentrations, 50 and 500 nM. No or little increase in cAMP binding under these two conditions would indicate that the binding sites were already close to saturation at 50 nM cAMP. The binding to truncated R/GFP fusions harbouring a functional site A (clones 34, 35 and 58 in Table 1) increased no more than 2.3 times, indicating a high affinity binding. It should be noted that the control R binding (100% in Tables 1 and 2) corresponded

to 40% of the subunits binding one molecule of cAMP. Thus, the 2.3 times increase obtained in clones 34 and 35 resulted in a total occupancy of the cAMP binding site. A similar increase was also observed for complete R/GFP fusion clones 101, 28, 89 and 33, although in these cases, only a fraction of the molecules were binding cAMP, possibly indicating a lower affinity than the previous group. In contrast, clones 20, 59 and 37 increased cAMP binding from five to 10 times when incubated at 500 nM cAMP as compared with 50 nM cAMP, indicating that the insertion of GFP resulted in a decrease of the affinity for cAMP. Extreme cases from this last group were clones 20 and 59, which presented a quasi-linear increase in binding up to the maximum concentration tested (800 nM cAMP). As a whole, these results provided evidence that the lower values of cAMP binding observed in a number of R/GFP fusion proteins could at least in part be due to lower affinities for cAMP.

We also verified that both cAMP binding and green fluorescence were carried by the same polypeptide since green fluorescence was retained on cAMP–agarose and eluted with cAMP (not shown). This eliminates the possibility that in a given extract, subpopulations of proteins with well-folded GFP but not having a functional R subunit would co-exist with others displaying cAMP binding but not
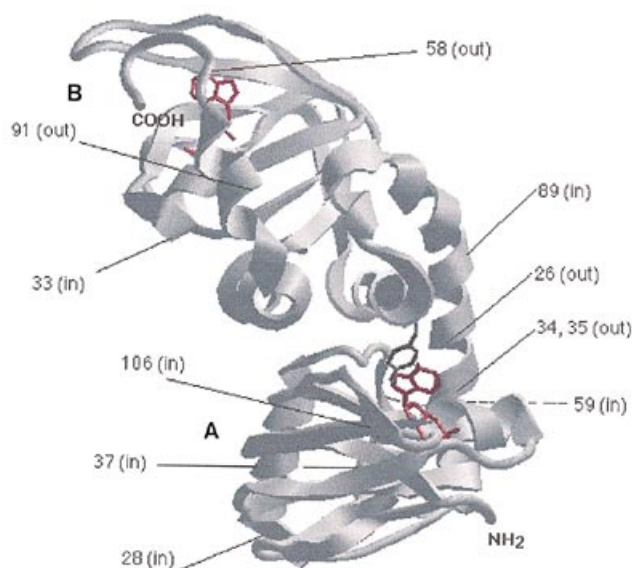
Figure 5. Model of the *Dictyostelium* R subunit showing GFP insertion sites. *Dictyostelium* R subunit with bound cAMP was modelled using the program Swiss-PdbViewer (18), based on the structure of the (Δ1–91) R subunit from mouse (14). Insertion sites are indicated by an arrow. (in) or (out) indicate that the C-terminus of the R subunit is in-frame or out of frame with the inserted GFP. cAMP bound to the R subunit are shown in solid sticks. Tyr197 is also shown. The cAMP binding sites A and B are indicated by homology to the structure presented in Su *et al.* (14).

having functional GFP. Clones 20, 37 and 59 did not bind cAMP–agarose, which is likely due to their lower affinity for cAMP.

Finally, we tested whether the R/GFP fusion proteins were able to inhibit PKA catalytic activity. From the 14 clones previously presented, only clones 91, 58 and 33 inhibited the PKA activity present in crude extracts of bacteria expressing the catalytic core (C309) of the C subunit (data not shown). In all three cases, inhibition was released by adding 50 μM cAMP. These results indicate that the R–C interaction is not impaired by insertion of GFP within the cAMP binding site B (Fig. 5), in agreement with previous reports showing that deletion of site B up to Trp260 has no effect on C subunit inhibition (15). The fact that R/GFP fusions 91, 58 and 33 show a different affinity for cAMP may allow sensitive measurement over a broad range of cAMP concentrations within the cell. In addition, our results underline the importance of the α-helix connecting cAMP binding sites A and B, since C-terminal deletions in clones 26, 34 and 35 result in a loss of interaction with the C subunit, despite an ability to bind cAMP. Clone 89, in which GFP is inserted in-frame, is impaired both in cAMP binding and R–C interaction, further indicating the essential role of the α-helix in between sites A and B.

In conclusion, we have developed a methodology for random insertion of GFP within the coding region of a protein of interest. This method enables the selection of fusion proteins where at least the GFP is functional. Further studies on the R/GFP clones indicated that, even though cAMP binding was lowered in many instances, indicating a potential lower affinity, binding was observed in all clones harbouring a GFP fused in-frame with the R subunit. Twenty per cent of the R/GFP fusions were able to interact with the C subunit *in vitro*. The lack of PKA inhibition by R subunits presenting a GFP insertion within the α-helix present at the end of the cAMP binding site A (clones 89, 26, 34 and 35)

further implicates a role for this region in the interaction between R and C subunits. These results indicate that random insertion of GFP can complement more thorough functional mapping.

GFP fusions at either ends of the R and C subunits from mammals or *Dictyostelium* have previously been performed, but no FRET could be measured (A.Kuspa and T.Pozzan, personal communication). Even though fully in-frame GFP insertion did not result in the isolation of R/GFP fusions having both high fluorescence and high affinity for cAMP, the progressive C-terminal deletions presented here offer a chance to place GFP in closer proximity to another mutant GFP on the C subunit. This process may provide a route to finally obtain intermolecular FRET in a two-component system. The knowledge that GFP can be randomly inserted while maintaining significant cAMP binding by the R subunit, indicates that this type of approach should also be possible for the C subunit. Furthermore, the methodology presented herein could widen the spectrum of approaches used to isolate partners for FRET and could further be applied to proteins for which a crystal structure is not yet available.

REFERENCES

1 Prasher,D.C., Eckenrode,V.K., Ward,W.W., Prendergast,F.G. and Cormier,M.J. (1992) *Gene*, **111**, 229–233.
2 Cubitt,A.B., Heim,R., Adams,S.R., Boyd,A.E., Gross,L.A. and Tsien,R.Y. (1995) *Trends Biochem. Sci.*, **20**, 448–455.
3 Chalfie,M., Tu,Y., Euskirchen,G., Ward,W.W. and Prasher,D.C. (1994) *Science*, **263**, 802–805.
4 Heim,R. and Tsien,R.Y. (1996) *Curr. Biol.*, **6**, 178–182.
5 Romoser,V.A., Hinkle,P.M. and Persechini,A. (1997) *J. Biol. Chem.*, **272**, 13270–13274.
6 Miyawaki,A., Llopis,J., Heim,R., McCaffery,J.M., Adams,J.A., Ikura,M. and Tsien,R. (1997) *Nature*, **388**, 882–887.
7 Ogreid,D., Ekanger,R., Suva,R.H., Miller,J.P. and Doskeland,S.O. (1989) *Eur. J. Biochem.*, **181**, 19–31.
8 Adams,S.R., Harootunian,A.T., Buechler,Y.J., Taylor,S. and Tsien,R. (1991) *Nature*, **349**, 694–697.
9 Mutzel,R., Lacombe,M.-L., Simon,M.-N., de Grunzburg,J. and Véron,M. (1987) *Proc. Natl Acad. Sci. USA*, **84**, 6–10.
10 Etchebehere,L.C., van Bemmelen,M.X., Anjard,C., Traincard,F., Assemat,K., Reymond,C. and Véron,M. (1997) *Eur. J. Biochem.*, **248**, 820–826.
11 Dammann,H., Traincard,F., Anjard,C., van Bemmelen,M.X.P., Reymond,C. and Véron,M. (1998) *Mech. Dev.*, **72**, 149–157.
12 Luckow,B., Renkawitz,R. and Schütz,G. (1987) *Nucleic Acids Res.*, **15**, 417–429.
13 Doskeland,S.O. and Ogreid,D. (1988) *Methods Enzymol.*, **159**, 147–150.
14 Su,Y., Dostmann,R.G., Herberg,F.W., Durick,K., Xuong,N.-h., Ten Eyck,L., Taylor,S.S. and Varughese,K.I. (1995) *Science*, **269**, 807–813.
15 Saraswat,L.D., Ringheim,G.E., Bubis,J. and Taylor,S.S. (1988) *J. Biol. Chem.*, **263**, 18241–18246.
16 Gorman,K.B. and Steinberg,R.A. (1994) *Somat. Cell Mol. Genet.*, **20**, 301–311.
17 Siegel,M.S. and Isacoff,E.Y. (1997) *Neuron*, **19**, 735–741.
18 Guex,N. and Peitsch,M.C. (1997) *Electrophoresis*, **18**, 2714–2723.